Article

Current Biology

A New Perspective on Ecological Prediction Reveals Limits to Climate Adaptation in a Temperate Tree Species

Highlights

- NSC stores in *P. trichocarpa* are heritable and locally adapted to climate
- Despite species-wide evolutionary potential in storage, populations are at risk
- Northern populations lack the genomic variants to evolve with climate change
- Southern populations have genomic diversity but face intense selective pressures

Authors

Meghan Blumstein, Andrew Richardson, David Weston, Jin Zhang, Wellington Muchero, Robin Hopkins

Correspondence

blumstein@fas.harvard.edu

In Brief

Blumstein et al. show variation in NSC storage in trees is heritable and locally adapted to climate. Despite species-wide evolutionary potential in storage, some populations are at risk. Northern populations lack genomic variants associated with high storage, while southern populations have these variants but face intense selective pressures.

Blumstein et al., 2020, Current Biology *30*, 1447–1453
April 20, 2020
https://doi.org/10.1016/j.cub.2020.02.001

CellPress

Current Biology
Article

A New Perspective on Ecological Prediction Reveals Limits to Climate Adaptation in a Temperate Tree Species

Meghan Blumstein,[1,6,*] Andrew Richardson,[2,3] David Weston,[4] Jin Zhang,[4] Wellington Muchero,[4] and Robin Hopkins[1,5]
[1]Department of Organismic and Evolutionary Biology, Harvard University, 26 Oxford Street, Cambridge, MA 02138, USA
[2]Center for Ecosystem Science and Society, Northern Arizona University, Flagstaff, AZ 86011, USA
[3]School of Informatics, Computing, and Cyber Systems, Northern Arizona University, Flagstaff, AZ 86011, USA
[4]Biosciences Division, Oak Ridge National Laboratory, Oak Ridge, TN 37831, USA
[5]The Arnold Arboretum, 1300 Centre Street, Boston, MA 02130, USA
[6]Lead Contact
*Correspondence: blumstein@fas.harvard.edu
https://doi.org/10.1016/j.cub.2020.02.001

SUMMARY

Forests absorb a large fraction of anthropogenic CO2 emission, but their ability to continue to act as a sink under climate change depends in part on plant species undergoing rapid adaptation. Yet models of forest response to climate change currently ignore local adaptation as a response mechanism. Thus, considering the evolution of intraspecific trait variation is necessary for reliable, long-term species and climate projections. Here, we combine ecophysiology and predictive climate modeling with analyses of genomic variation to determine whether sugar and starch storage, energy reserves for trees under extreme conditions, have the heritable variation and genetic diversity necessary to evolve in response to climate change within populations of black cottonwood (*Populus trichocarpa*). Despite current patterns of local adaptation and extensive range-wide heritable variation in storage, we demonstrate that adaptive evolution in response to climate change will be limited by a lack of heritable variation within northern populations and by a need for extreme genetic changes in southern populations. Our method can help design more targeted species management interventions and highlights the power of using genomic tools in ecological prediction to scale from molecular to regional processes to determine the ability of a species to respond to future climates.

INTRODUCTION

Rates of forest tree mortality are increasing across large regions of the globe as a result of shifting drought regimes, extreme temperatures, and pest outbreaks associated with global change [1–4]. The rise in number and intensity of these climate-related selective pressures means adaptive evolution from local standing heritable variation will be a core component of species persistence strategies, along with migration and acclimation via plasticity [5, 6]. Adaptive evolution is particularly important, as tree populations already exhibit a high degree of local adaptation [7–9]. Despite high gene flow and long generation times [10], tree populations are able to undergo rapid adaptation, as evidenced by the paleoecological record following glaciation [11, 12]. Furthermore, plasticity and migration are unlikely to keep pace with climate change. Plastic variation may help plants temporarily acclimate to new climates, but studies have demonstrated that plastic variation may not be enough to cope with predicted change [13, 14] or may even be maladaptive [15]. In addition, migration rates may be limited due to dispersal rates and dispersal barriers [16, 17]. Thus, adaptation is a critical pillar of plant response to climate yet one that is often ignored in our species projections, despite its demonstrated improvement of models [18, 19].

Adaptive response is dependent on both the extent of heritable variation underlying an adaptive trait as well as the magnitude of evolutionary change necessary to meet the demands of unprecedented environmental change. Therefore, adaptive alleles must both be present in a population and be at appreciable allele frequencies to allow rapid evolution in response to rising temperatures and shifting precipitation patterns. Without the intraspecific trait variation necessary to evolve, populations will be at risk of local extinction [20–22]. To predict whether a species will be able to adapt to future climate, we must first identify a trait that is in fact adaptive, second quantify the amount and geographic distribution of heritable variation in the trait, third identify the genomic loci and subsequent alleles underlying the trait, and fourth assess the potential for these alleles to undergo local adaptive evolution [6, 9, 23, 24]. Here, we take these four steps to determine the potential for black cottonwood (*Populus trichocarpa*) to adapt to climate change through the evolution of variation in sugar and starch storage, hereafter referred to as nonstructural carbohydrate (NSC) storage.

The storage of NSCs has been hypothesized to be a key trait in providing resilience to trees under stress [25–27]. NSCs are labile sugars and starches stored in the parenchyma cells of woody tissues (stems, roots, etc.) in plants [28, 29]. They can be stored on the order of days to decades and support metabolic processes in the dormant season as well as initiate leaf out in the spring

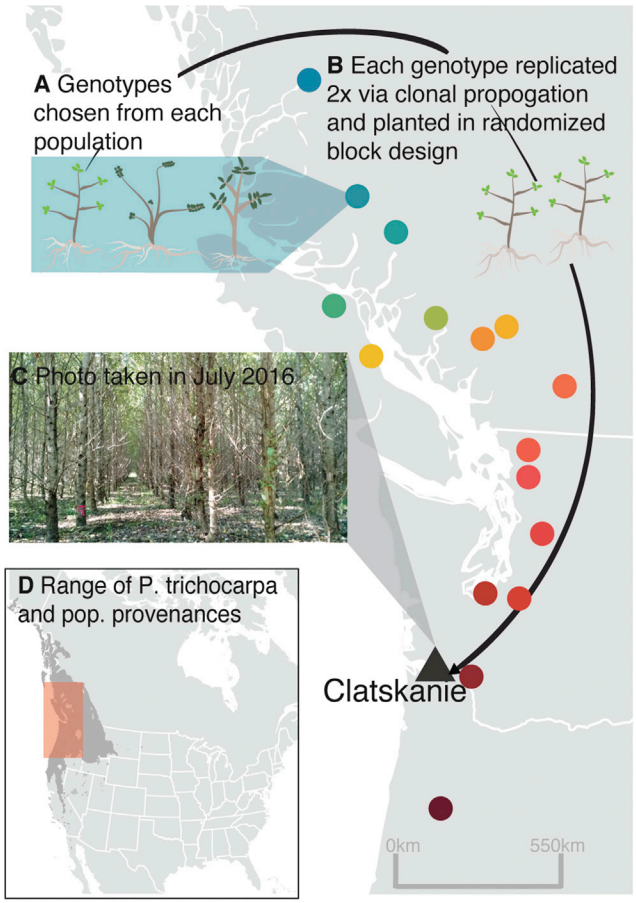

Figure 1. Common Garden Study Design

(A–C) Genotypes were (A) taken from each of 16 populations and (B) replicated twice via clonal propagation before being planted out in randomized blocks in the garden in Clatskanie, OR, as pictured in (C). Populations are color coded from cool to warm along a north-south axis.

(D) A map depicting the range of black cottonwood (*Populus trichocarpa*) and the subset of the range from which ramets were collected for planting in the common garden (black triangle).

[30]. NSC storage has also recently been thought to serve as a long-term "savings bank" for trees by allowing them to store energy in excess of their base demands in case future environmental extremes limit photosynthesis [25–27]. Under this hypothesis, plants would store more NSCs than needed in a normal year, which then act as an osmotic metabolic or defense buffer for trees growing in more stressful environments [26, 31]. Thus, plants growing in variable or extreme environments would be predicted to be locally adapted to store more than their counterparts in more ideal environments.

Recent studies on NSC storage have focused on the question of whether or not plants can tap into their stores and prolong life under stress. Many experimental and observational drought [32–34] and defoliation studies [35, 36] have demonstrated that plants can indeed draw down their NSC reserves under stress to sustain life under certain conditions (i.e., drought or shade), although some results are equivocal [37]. In addition, an experimental study of 10 tropical species has demonstrated a positive relationship between NSC storage and survival under drought, demonstrating that individuals who store *more* NSCs had higher stem water potentials and lived longer under stress [27]. Finally, interspecific studies indicate that average NSC storage can differ by up to 100% between species, indicating a potential genetic basis for the trait [38]. Together, these studies demonstrate that NSC stores, and more of them, can confer resilience under similar photosynthetically limiting stress, as predicted with climate change. However, no study to date has looked at variation within a species or across populations.

To evaluate the extent to which NSC storage is locally adapted and can continue to evolve in response to rapid climate change, we used a Department of Energy (DOE) common garden of black cottonwood (*Populus trichocarpa*) in Eastern Oregon [39]. We sampled both aboveground (stem) and belowground (root) woody tissues from 316 individuals, representing 242 genotypes and 16 populations (Figure 1), to measure heritable variation in NSC storage and find loci associated with the trait. We sampled during the dormant season (January), when the phloem is largely inactive [40, 41] and NSC variation is not impacted by variable fresh photosynthates. We then used the larger dataset of 860 resequenced genomes across 16 populations to make inferences about the evolutionary potential of NSC storage [39, 42].

RESULTS AND DISCUSSION

NSC Storage Is Heritable

Black cottonwoods have the NSC storage variation necessary for adaptive evolution. There is extensive total and heritable variation in aboveground (mean = 15.6 $mg \cdot g^{-1}$; σ_{Total} = 6.0 $mg \cdot g^{-1}$ NSC; $\sigma_{Heritable}$ = 2.8 $mg \cdot g^{-1}$ NSC) and belowground tissues (mean = 24.3 $mg \cdot g^{-1}$; σ_{Total} = 10.0 $mg \cdot g^{-1}$ NSC; $\sigma_{Heritable}$ = 3.6 $mg \cdot g^{-1}$ NSC). Roots store, on average, 1.6 ± 0.3 times higher concentrations of NSCs, which is consistent with other studies [38, 43]. By comparing genetic to total variation, we demonstrate significant broad-sense heritability underlying both aboveground and belowground NSC storage concentrations (Figure 1; $H^2_{aboveground}$ = 0.43 ± 0.1; $H^2_{belowground}$ = 0.32 ± 0.1), indicating that approximately 1/3 to 1/2 of variation measured in the garden could be passed onto offspring. NSC heritability is higher than most other physiological traits measured in the garden ($H^2_{Physiology\ Traits}$ = 0.26 ± 0.18) [44] and is on par with other traits thought to be associated with climate adaptation, such as relative growth rate (H^2_{Growth} = 0.42 ± 0.1). However, we found no heritability of variation in the ratio of above- to belowground storage concentrations ($H^2_{A/B}$ = 0.04 ± 0.0).

The amount of heritable variation in NSC storage is notable, with ranges spanning several percentage points for both aboveground (0.5%–3%; Δ 2.5%) and belowground (1%–4%; Δ 3%) storage. This variation is biologically meaningful, as even a 2%–4% increase in NSC storage can prolong lifespan of tree seedlings up to 9 days under experimental drought conditions [27]. Black cottonwood trees are riverine species and highly sensitive to changes in water level [45, 46], and Northwestern North America is projected to become drier over the next 100 years, with a significant decrease in the snowpack and precipitation that maintains river water levels [47]. Thus, the ability to evolve higher NSC storage concentrations as a back-up fuel source

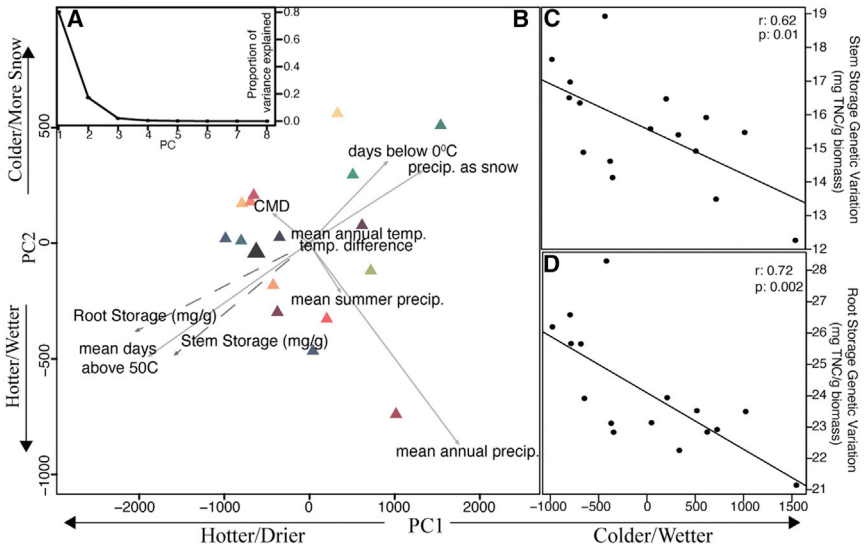

Figure 2. Population-Level Genetic Variation in NSC Storage Compared to the Climate of Origin

(A) A principle components analysis (PCA) of climate variables; the majority of the variance (81%) among site climate variables can be explained by PC1.

(B) Climate variables represent 30-year normal of parameters describing dryness and temperature, with PC1 largely indicating a gradient from wet and cool in the positive values to hot and dry in the negative range, although PC2 represents a gradient from warm and wet in the negative values to cold and dry in the positive values. Each population's current climate (triangle) and the site of the common garden (large gray triangle) are indicated. Population color varies from red in the South to blue in the North as in Figure 1.

(C and D) The results of a correlation analysis between PC1 and (C) above- and (D) belowground population-level heritable variation in NSC storage concentrations are presented on the right.

or a pool for maintaining hydraulic function could be a crucial survival trait for trees [48].

Climate Shapes NSC Storage

To determine the extent to which variation in NSCs are locally adapted and shaped by selection, we compare the heritable trait variation to the neutral genetic variation across populations. Specifically, we calculate the quantitative genetic trait differentiation among populations (Q_{st}) and compared this to the genomic differentiation at neutral sites among populations (F_{st}) [49] (mean; 95% credible interval; aboveground: Q_{st} = 0.31, 0.12–0.56; belowground: Q_{st} = 0.30, 0.11–0.57; [mean ± SD] F_{st} = 0.17 ± 0.06). Among populations, NSC storage variation significantly exceeds background genomic variation in both above and belowground NSC storage, supporting that divergence in NSC storage between populations is driven by natural selection (Wilcoxon test; aboveground: W = 18,675,000, $p < 0.001$; belowground: W = 17,894,000, $p < 0.001$).

Heritable variation in NSC storage is highly correlated with major environmental gradients across the range of black cottonwood, indicating local adaptation. We used a principal-component analysis (PCA) to reduce the dimensionality of and control for collinearity among relevant climate variables (Figures 2 and 3). The first PC describes an axis of colder/wetter to hotter/drier climates and is significantly correlated with heritable variation in both above- and belowground NSC storage (Figures 2 and 3; aboveground: d.f. = 14, r = 0.62, p = 0.01; belowground: d.f. = 14, r = 0.72, p = 0.002).

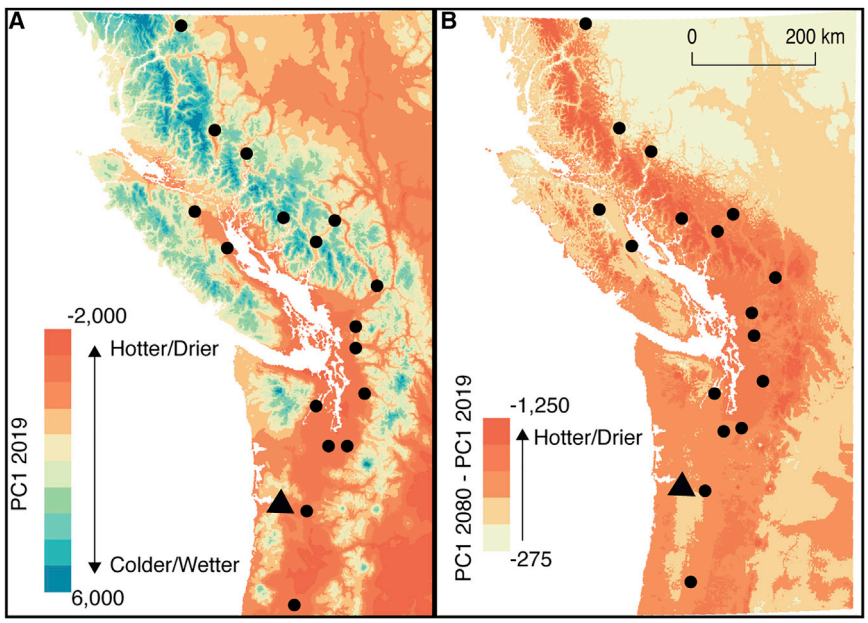

Figure 3. Current and Future Climate of Western North America Mapped in PC1 Space

Maps of (A) climatic variation along PC1 of present-day climate (2019) and (B) the difference along the climatic PC1 axis between the CCSM3 A1B future climate projections (2080) and the present-day climate. Dots represent populations, and the triangle is the location of the common garden in Clatskanie. The entire region is predicted to move in the more negative direction along PC1 (i.e., hotter and drier), with larger changes (darker color) occurring at high elevation and more southerly sites.

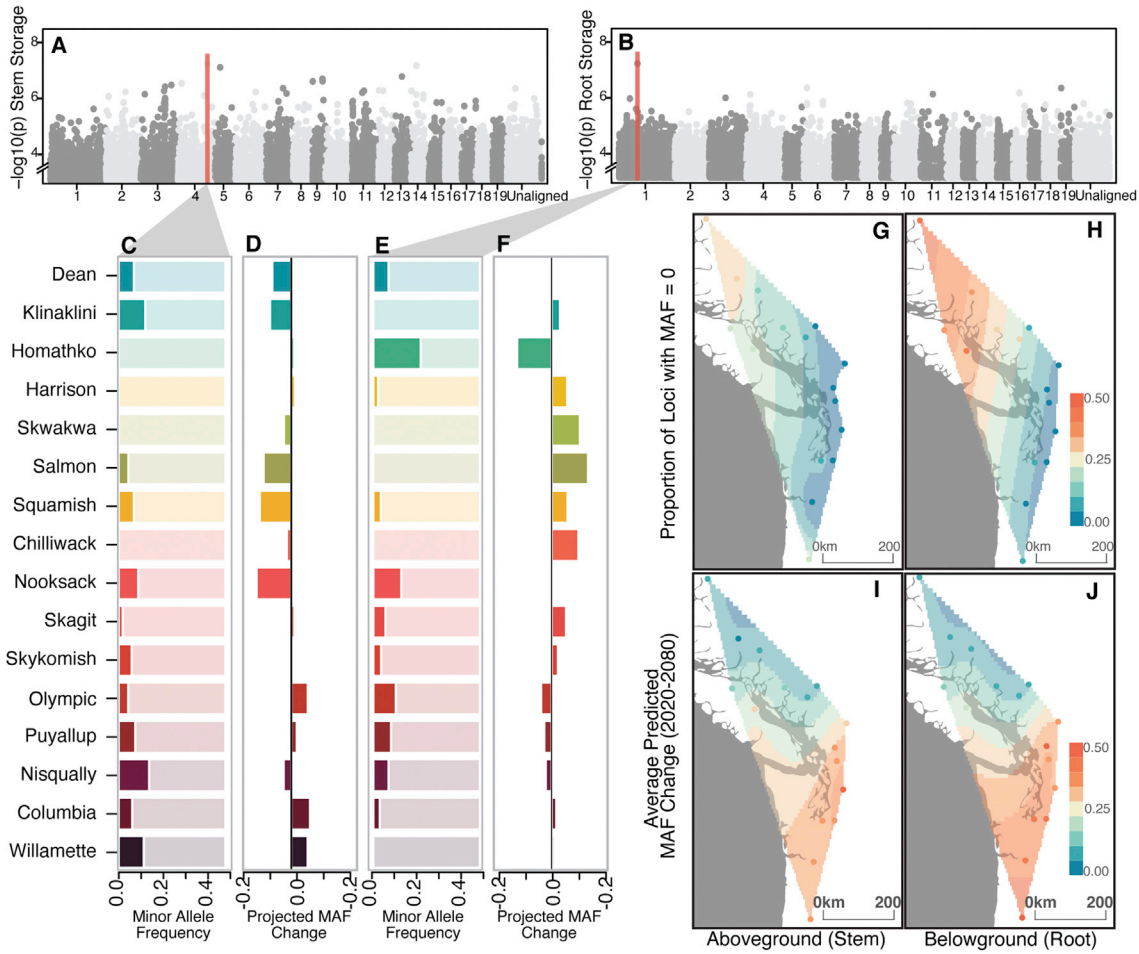

Figure 4. Using GWAS Results to Assess Adaptive Potential

(A and B) Genome-wide analysis study (GWAS) results for (A) aboveground and (B) belowground total NSC storage.

(C–F) The minor allele frequency (MAF) for the most significant loci in each GWAS (highlighted via a red line) is plotted for each population and 1,060 genomes (C and E), with the plots directly adjacent (D and F) showing the predicted change in MAF over the next 60 years due to climate change (IPCC A1B scenario).

(G and H) The top row of maps illustrate the proportion of loci associated with (G) aboveground and (H) belowground NSC storage that entirely lack the minor allele altogether (e.g., plot C and plot E; population Skwakwa), with warm colors lacking heritable variation. The bottom row of maps illustrates the average amount of absolute MAF change predicted under future climate scenarios, with warmer colors requiring greater allele frequency shifts.

See also Table S1 and Figures S2 and S4.

Individuals originating from hotter-drier environments have greater storage, lending support to the hypothesized relationship between environmental stress and NSC storage [25, 32], although, in black cottonwood, it is difficult to isolate the effect of latitude and subsequently phenological timing from climate. Further, NSC variation is largely uncorrelated with heritable variation in stem diameter (Figure S1; aboveground: m = 0.02, r = 0.13, p = 0.15; belowground: m = 0.03, r = 0.22, p = 0.04), suggesting that storage is genetically independent of growth. The geographic patterns of heritable variation in NSC storage are consistent with trees living at the extreme edge of their environmental tolerance evolving an adaptive "bet-hedging" strategy, although additional experiments teasing apart climate variables, mean versus variance in climate metrics, and phenology are needed to hone in on the precise climate drivers of local adaptation in storage.

Low Evolutionary Potential under Climate Change due to Allele Frequency Distributions

Given the existence of heritable variation in NSC storage, we used a genome-wide association study (GWAS) to identify candidate loci underlying storage. We find 209 SNPs above our inclusion cutoff from 111 genes associated with aboveground NSC storage and 86 SNPs from 50 genes associated with belowground storage (Figure 4A, 4B, and S2). Aboveground loci are enriched for several biological and molecular process gene ontology (GO) terms, such as carbohydrate metabolic process and catalytic activity, although belowground loci are enriched in functions such as transport (Figure S3). In both analyses, several genes associated with carbohydrate synthesis and transport were highlighted by our analysis (Table S1). All subsequent analyses were replicated using both the complete set of associated SNPs as well as a representative candidate

SNP for each unique gene; both show qualitatively similar results.

Our goal is to determine whether there is available local heritable variation at loci associated with variation in NSC storage that will allow for rapid evolution in response to climate change. We assess the current distribution of allele frequencies across populations by calculating the minor allele frequency (MAF), or proportion of individuals with the less common allele, within each population for each locus associated with aboveground or belowground NSC storage. This analysis uses the full DOE set of 860 resequenced black cottonwood genomes. We then transform our 30-year climate normal data, which represent the current conditions, into PC space and statistically associate the climate with population-level allele frequencies using a canonical-correlation analysis (CCA), which tests associations between two sets of multivariate variables [50] (Figure 3). We used the correlations between allele frequency and current climate to predict allele patterns under future climate conditions. Specifically, we used 2,080 projected climate conditions [47] transformed into PC space for each of our sampled populations to predict the expected MAF at each locus that would allow for current levels of local adaptation under future conditions (e.g., Figure 4C–4F; IPCC A1B scenario, CSM4 model). We also found our results to be robust to other climate models (Figure S4; IPCC A1B, CMIP3 23 model ensemble).

Populations at the edges of the black cottonwood range are vulnerable to extinction over the next 60 years due to insufficient heritable variation required for adaptive evolution to climate change. At the northern range limit, populations are entirely missing alleles associated with greater storage; up to 50% of loci within a population lack the allelic variation necessary to respond to warmer and drier climates (Figure 4G and 4H). This is concerning, given evidence that migration is unlikely to keep pace with rapid warming [16, 17]. However, our results do present opportunities for genetic rescue by identifying the target populations and alleles for use in assisted migration. Genetic rescue, or the migration of adaptive alleles into a population, has enabled rapid adaptation in several animal species (reviewed in [51]), and an assisted migration program is already in effect for the tree species larch [52].

In contrast, southern populations tend to contain the alleles associated with warmer/drier conditions, but these populations require extreme changes in allele frequency to adapt to future climate conditions. MAFs at populations below 50° latitude are predicted to shift in frequency Δ0.25–0.5 on average, although northern populations' frequencies are only projected to shift Δ0.03–0.12 on average (Figure 4I and 4J). The cost of the required selection in southern populations could result in local extinctions, as the number of individuals that may die could cause populations to drop below sustainable numbers [20, 22, 53, 54]. If the size of a population is reduced below a critical level, it becomes highly susceptible to extinction by demographic stochasticity, even if the genetic capacity to adapt to new environmental conditions is present in the population [20, 22, 53]. Given the rapidity of change is likely to outstrip generation time in *populus* (10–15 years to reproductive maturity), phenotypic plasticity may be key in ameliorating the short-term impacts of climate selection on southern populations [55, 56]. Future studies should examine the degree of plasticity in NSC storage and the environmental conditions that may induce higher storage.

Conclusions

We demonstrate the power of incorporating genomic data and an evolutionary perspective with plant physiology to scale from molecular measurements to regional predictions and thus better understand species response to climate change. Black cottonwood populations have locally adapted to climate through variation in NSC storage. However, despite extensive range-wide heritable intraspecific variation in storage, a lack of allelic variation locally will significantly limit the ability of this species to rapidly evolve in response to climate change. We reveal nuances in what is required for adaptation to occur across the range of a species that should inform how we design species management interventions and bring a new perspective to ecological prediction.

STAR★METHODS

Detailed methods are provided in the online version of this paper and include the following:

- KEY RESOURCES TABLE
- LEAD CONTACT AND MATERIALS AVAILABILITY
- EXPERIMENTAL MODEL AND SUBJECT DETAILS
- METHOD DETAILS
  - Field Collection
  - NSC Laboratory Preparation
- QUANTIFICATION AND STATISTICAL ANALYSIS
  - Spatial Autocorrelation
  - Statistical Model
  - Heritability, Q_{st}, and F_{st}
  - Climate
  - Genome-Wide Association Study & Gene Ontology
  - Minor Allele Frequency Projections
- DATA AND CODE AVAILABILITY

SUPPLEMENTAL INFORMATION

Supplemental Information can be found online at https://doi.org/10.1016/j.cub.2020.02.001.

ACKNOWLEDGMENTS

We thank M.E. Furze, C.F. White, D.L. Des Marais, N.M. Holbrook, and N. Freidman for comments and A. Viser, L. Gunter, E. Borjigin-Wang, and A. Chan for lab assistance. This material is based upon work supported by the US Department of Energy, Office of Science, Office of Workforce Development for Teachers and Scientists, Office of Science Graduate Student Research (SCGSR) program; by the National Science Foundation Graduate Research Fellowship under grant no. DGE1745303; and the Explorer's Club. The SCGSR program is administered by the Oak Ridge Institute for Science and Education (ORISE) for the DOE. ORISE is managed by ORAU under contract number DE-SC0014664.

AUTHOR CONTRIBUTIONS

Conceptualization, M.B., A.R., and R.H.; Data Collection/Processing, M.B., GWAS, J.Z., and W.M.; Statistical Analysis and Modeling, M.B.; Writing, M.B. and R.H.; Review and Editing, M.B., A.R., D.W., J.Z., W.M., and R.H.

DECLARATION OF INTERESTS

The authors declare no competing interests.

Received: October 29, 2019
Revised: December 17, 2019
Accepted: February 3, 2020
Published: March 26, 2020

REFERENCES

1. Allen, C.D., Macalady, A.K., Chenchouni, H., Bachelet, D., McDowell, N., Vennetier, M., Kitzberger, T., Rigling, A., Breshears, D.D., Hogg, E.H., et al. (2010). A global overview of drought and heat-induced tree mortality reveals emerging climate change risks for forests. For. Ecol. Manage. *259*, 660–684.
2. McDowell, N., Allen, C.D., Anderson-Teixeira, K., Brando, P., Brienen, R., Chambers, J., Christoffersen, B., Davies, S., Doughty, C., Duque, A., et al. (2018). Drivers and mechanisms of tree mortality in moist tropical forests. New Phytol. *219*, 851–869.
3. Anderegg, W.R., Hicke, J.A., Fisher, R.A., Allen, C.D., Aukema, J., Bentz, B., Hood, S., Lichstein, J.W., Macalady, A.K., McDowell, N., et al. (2015). Tree mortality from drought, insects, and their interactions in a changing climate. New Phytol. *208*, 674–683.
4. Anderegg, W.R., Klein, T., Bartlett, M., Sack, L., Pellegrini, A.F., Choat, B., and Jansen, S. (2016). Meta-analysis reveals that hydraulic traits explain cross-species patterns of drought-induced tree mortality across the globe. Proc. Natl. Acad. Sci. USA *113*, 5024–5029.
5. Aitken, S.N., Yeaman, S., Holliday, J.A., Wang, T., and Curtis-McLane, S. (2008). Adaptation, migration or extirpation: climate change outcomes for tree populations. Evol. Appl. *1*, 95–111.
6. Sork, V.L., Aitken, S.N., Dyer, R.J., Eckert, A.J., Legendre, P., and Neale, D.B. (2013). Putting the landscape into the genomics of trees: approaches for understanding local adaptation and population responses to changing climate. Tree Genet. Genomes *9*, 901–911.
7. Savolainen, O., Pyhäjärvi, T., and Knürr, T. (2007). Gene flow and local adaptation in trees. Annu. Rev. Ecol. Evol. Syst. *38*, 595–619.
8. Borkowski, D.S., Hoban, S.M., Chatwin, W., and Romero-Severson, J. (2017). Rangewide population differentiation and population substructure in *Quercus rubra* L. Tree Genet. Genomes *13*, 67.
9. Alberto, F.J., Aitken, S.N., Alía, R., González-Martínez, S.C., Hänninen, H., Kremer, A., Lefèvre, F., Lenormand, T., Yeaman, S., Whetten, R., and Savolainen, O. (2013). Potential for evolutionary responses to climate change - evidence from tree populations. Glob. Change Biol. *19*, 1645–1661.
10. Kremer, A., Ronce, O., Robledo-Arnuncio, J.J., Guillaume, F., Bohrer, G., Nathan, R., Bridle, J.R., Gomulkiewicz, R., Klein, E.K., Ritland, K., et al. (2012). Long-distance gene flow and adaptation of forest trees to rapid climate change. Ecol. Lett. *15*, 378–392.
11. Davis, M.B., and Shaw, R.G. (2001). Range shifts and adaptive responses to Quaternary climate change. Science *292*, 673–679.
12. Davis, M.B., Shaw, R.G., and Etterson, J.R. (2005). Evolutionary responses to changing climate. Ecology *86*, 1704–1714.
13. Duputié, A., Rutschmann, A., Ronce, O., and Chuine, I. (2015). Phenological plasticity will not help all species adapt to climate change. Glob. Change Biol. *21*, 3062–3073.
14. Franks, S.J. (2011). Plasticity and evolution in drought avoidance and escape in the annual plant Brassica rapa. New Phytol. *190*, 249–257.
15. Hendry, A.P. (2016). Key questions on the role of phenotypic plasticity in eco-evolutionary dynamics. J. Hered. *107*, 25–41.
16. Zhu, K., Woodall, C.W., and Clark, J.S. (2012). Failure to migrate: lack of tree range expansion in response to climate change. Glob. Change Biol. *18*, 1042–1052.
17. McLachlan, J.S., Clark, J.S., and Manos, P.S. (2005). Molecular indicators of tree migration capacity under rapid climate change. Ecology *86*, 2088–2098.
18. Cotto, O., Wessely, J., Georges, D., Klonner, G., Schmid, M., Dullinger, S., Thuiller, W., and Guillaume, F. (2017). A dynamic eco-evolutionary model predicts slow response of alpine plants to climate warming. Nat. Commun. *8*, 15399.
19. Valladares, F., Matesanz, S., Guilhaumon, F., Araújo, M.B., Balaguer, L., Benito-Garzón, M., Cornwell, W., Gianoli, E., van Kleunen, M., Naya, D.E., et al. (2014). The effects of phenotypic plasticity and local adaptation on forecasts of species range shifts under climate change. Ecol. Lett. *17*, 1351–1364.
20. Allaby, R.G., Kitchen, J.L., and Fuller, D.Q. (2016). Surprisingly low limits of selection in plant domestication. Evol. Bioinform. Online *11* (*Suppl 2*), 41–51.
21. Polechová, J., and Barton, N.H. (2015). Limits to adaptation along environmental gradients. Proc. Natl. Acad. Sci. USA *112*, 6401–6406.
22. Smith, J.M. (1968). "Haldane's dilemma" and the rate of evolution. Nature *219*, 1114–1116.
23. Anderson, J.T., Inouye, D.W., McKinney, A.M., Colautti, R.I., and Mitchell-Olds, T. (2012). Phenotypic plasticity and adaptive evolution contribute to advancing flowering phenology in response to climate change. Proc. Biol. Sci. *279*, 3843–3852.
24. Anderegg, W.R.L. (2015). Spatial and temporal variation in plant hydraulic traits and their relevance for climate change impacts on vegetation. New Phytol. *205*, 1008–1014.
25. McDowell, N., Pockman, W.T., Allen, C.D., Breshears, D.D., Cobb, N., Kolb, T., Plaut, J., Sperry, J., West, A., Williams, D.G., and Yepez, E.A. (2008). Mechanisms of plant survival and mortality during drought: why do some plants survive while others succumb to drought? New Phytol. *178*, 719–739.
26. Sala, A., Piper, F., and Hoch, G. (2010). Physiological mechanisms of drought-induced tree mortality are far from being resolved. New Phytol. *186*, 274–281.
27. O'Brien, M.J., Reynolds, G., Ong, R., and Hector, A. (2017). Resistance of tropical seedlings to drought is mediated by neighbourhood diversity. Nat. Ecol. Evol. *1*, 1643–1648.
28. Chapin, F.S., III, Schulze, E., and Mooney, H.A. (1990). The ecology and economics of storage in plants. Annu. Rev. Ecol. Syst. *21*, 423–447.
29. Plavcová, L., and Jansen, S. (2015). The role of xylem parenchyma in the storage and utilization of nonstructural carbohydrates. In Functional and Ecological Xylem Anatomy, U. Hacke, ed. (Springer), pp. 209–234.
30. Hartmann, H., and Trumbore, S. (2016). Understanding the roles of nonstructural carbohydrates in forest trees - from what we can measure to what we want to know. New Phytol. *211*, 386–403.
31. McDowell, N.G., and Sevanto, S. (2010). The mechanisms of carbon starvation: how, when, or does it even occur at all? New Phytol. *186*, 264–266.
32. Sevanto, S., McDowell, N.G., Dickman, L.T., Pangle, R., and Pockman, W.T. (2014). How do trees die? A test of the hydraulic failure and carbon starvation hypotheses. Plant Cell Environ. *37*, 153–161.
33. Quirk, J., McDowell, N.G., Leake, J.R., Hudson, P.J., and Beerling, D.J. (2013). Increased susceptibility to drought-induced mortality in Sequoia sempervirens (Cupressaceae) trees under Cenozoic atmospheric carbon dioxide starvation. Am. J. Bot. *100*, 582–591.
34. Hartmann, H., Ziegler, W., and Trumbore, S. (2013). Lethal drought leads to reduction in nonstructural carbohydrates in Norway spruce tree roots but not in the canopy. Funct. Ecol. *27*, 413–427.
35. Landhäusser, S.M., and Lieffers, V.J. (2012). Defoliation increases risk of carbon starvation in root systems of mature aspen. Trees *26*, 653–661.
36. Piper, F.I., and Fajardo, A. (2014). Foliar habit, tolerance to defoliation and their link to carbon and nitrogen storage. J. Ecol. *102*, 1101–1111.

37. Adams, H.D., Zeppel, M.J.B., Anderegg, W.R.L., Hartmann, H., Landhäusser, S.M., Tissue, D.T., Huxman, T.E., Hudson, P.J., Franz, T.E., Allen, C.D., et al. (2017). A multi-species synthesis of physiological mechanisms in drought-induced tree mortality. Nat. Ecol. Evol. *1*, 1285–1291.

38. Furze, M.E., Huggett, B.A., Aubrecht, D.M., Stolz, C.D., Carbone, M.S., and Richardson, A.D. (2019). Whole-tree nonstructural carbohydrate storage and seasonal dynamics in five temperate species. New Phytol. *221*, 1466–1477.

39. Slavov, G.T., DiFazio, S.P., Martin, J., Schackwitz, W., Muchero, W., Rodgers-Melnick, E., Lipphardt, M.F., Pennacchio, C.P., Hellsten, U., Pennacchio, L.A., et al. (2012). Genome resequencing reveals multiscale geographic structure and extensive linkage disequilibrium in the forest tree Populus trichocarpa. New Phytol. *196*, 713–725.

40. Aloni, R., Raviv, A., and Peterson, C.A. (1991). The role of auxin in the removal of dormancy callose and resumption of phloem activity in *Vitis vinifera*. Can. J. Bot. *69*, 1825–1832.

41. Bowen, M.R., and Hoad, G.V. (1968). Inhibitor content of phloem and xylem sap obtained from willow (Salix viminalis L.) entering dormancy. Planta *81*, 64–70.

42. Tuskan, G.A., Difazio, S., Jansson, S., Bohlmann, J., Grigoriev, I., Hellsten, U., Putnam, N., Ralph, S., Rombauts, S., Salamov, A., et al. (2006). The genome of black cottonwood, Populus trichocarpa (Torr. & Gray). Science *313*, 1596–1604.

43. Richardson, A.D., Carbone, M.S., Keenan, T.F., Czimczik, C.I., Hollinger, D.Y., Murakami, P., Schaberg, P.G., and Xu, X. (2013). Seasonal dynamics and age of stemwood nonstructural carbohydrates in temperate forest trees. New Phytol. *197*, 850–861.

44. McKown, A.D., Guy, R.D., Klápště, J., Geraldes, A., Friedmann, M., Cronk, Q.C., El-Kassaby, Y.A., Mansfield, S.D., and Douglas, C.J. (2014). Geographical and environmental gradients shape phenotypic trait variation and genetic structure in Populus trichocarpa. New Phytol. *201*, 1263–1276.

45. Rood, S.B., Braatne, J.H., and Hughes, F.M. (2003). Ecophysiology of riparian cottonwoods: stream flow dependency, water relations and restoration. Tree Physiol. *23*, 1113–1124.

46. Rood, S.B., and Mahoney, J.M. (1990). Collapse of riparian poplar forests downstream from dams in western praries: probable causes and prospects for mitigation. Environ. Manage. *14*, 451–464.

47. IPCC (2013). Climate Change 2013: The Physical Science Basis. Contribution of Working Group I to the Fifth Assessment Report of the Intergovernmental Panel on Climate Change (Cambridge University Press).

48. Sala, A., Woodruff, D.R., and Meinzer, F.C. (2012). Carbon dynamics in trees: feast or famine? Tree Physiol. *32*, 764–775.

49. Whitlock, M.C., and Gilbert, K.J. (2012). Q(ST) in a hierarchically structured population. Mol. Ecol. Resour. *12*, 481–483.

50. Hamann, A., Wang, T., Spittlehouse, D.L., and Murdock, T.Q. (2013). A comprehensive, high-resolution database of historical and projected climate surfaces for western North America. Bull. Am. Meteorol. Soc. *94*, 1307–1309.

51. Whiteley, A.R., Fitzpatrick, S.W., Funk, W.C., and Tallmon, D.A. (2015). Genetic rescue to the rescue. Trends Ecol. Evol. *30*, 42–49.

52. O'Neill, G.A., Ukrainetz, N.K., Carlson, M., Cartwright, C.V., Jaquish, B.C., King, J.N., Krakowski, J., Russell, J.H., Stoehr, M.U., Xie, C.-Y., et al. (2008). Assisted migration to address climate change in British Columbia: recommendations for interim seed transfer standards. Volume Tech. Rep. *48*, B.C. Ministry of Forestry.

53. Haldane, J.B.S. (1957). The cost of natural selection. J. Genet. *55*, 511–524.

54. Lindsey, H.A., Gallie, J., Taylor, S., and Kerr, B. (2013). Evolutionary rescue from extinction is contingent on a lower rate of environmental change. Nature *494*, 463–467.

55. O'Connor, M.I., Selig, E.R., Pinsky, M.L., and Altermatt, F. (2012). Toward a conceptual synthesis for climate change responses. Glob. Ecol. Biogeogr. *21*, 693–703.

56. Matesanz, S., Gianoli, E., and Valladares, F. (2010). Global change and the evolution of phenotypic plasticity in plants. Ann. N Y Acad. Sci. *1206*, 35–55.

57. R Core Development Team (2018). R: A language and environment for statistical computing (R Foundation for Statistical Computing).

58. Zhang, J., Yang, Y., Zheng, K., Xie, M., Feng, K., Jawdy, S.S., Gunter, L.E., Ranjan, P., Singan, V.R., Engle, N., et al. (2018). Genome-wide association studies and expression-based quantitative trait loci analyses reveal roles of HCT2 in caffeoylquinic acid biosynthesis and its regulation by defense-responsive transcription factors in Populus. New Phytol. *220*, 502–516.

59. Carpenter, B., Gelman, A., Hoffman, M.D., Lee, D., Goodrich, B., Betancourt, M., Brubaker, M., Guo, J., Li, P., and Riddell, A. (2017). Stan: a probabalistic programming language. J. Stat. Softw. *76*, 1–32.

60. Oksanen, J., Blanchet, F.G., Friendly, M., Kindt, R., Legendre, P., McGlinn, D., Minchin, P.R., O'Hara, R.B., Simpson, G.L., Solymos, P., et al. (2019). vegan: Community Ecology Package. https://cran.r-project.org/web/packages/vegan/index.html.

61. Nychka, D., Furrer, R., Paige, J., and Sain, S. (2017). fields: Tools for spatial data (University Corporation for Atmospheric Research).

62. Alexa, A., and Rahnenfuhrer, J. (2019). topGO: Enrichment analysis for gene ontology. https://bioconductor.org/packages/release/bioc/html/topGO.html.

63. Falcon, S., and Gentleman, R. (2007). Using GOstats to test gene lists for GO term association. Bioinformatics *23*, 257–258.

64. Evans, L.M., Slavov, G.T., Rodgers-Melnick, E., Martin, J., Ranjan, P., Muchero, W., Brunner, A.M., Schackwitz, W., Gunter, L., Chen, J.G., et al. (2014). Population genomics of Populus trichocarpa identifies signatures of selection and adaptive trait associations. Nat. Genet. *46*, 1089–1096.

65. Richardson, A.D., Carbone, M.S., Huggett, B.A., Furze, M.E., Czimczik, C.I., Walker, J.C., Xu, X., Schaberg, P.G., and Murakami, P. (2015). Distribution and mixing of old and new nonstructural carbon in two temperate trees. New Phytol. *206*, 590–597.

66. Tixier, A., Orozco, J., Roxas, A.A., Earles, J.M., and Zwieniecki, M.A. (2018). Diurnal variation in nonstructural carbohydrate storage in trees: remobilization and vertical mixing. Plant Physiol. *178*, 1602–1613.

67. Chow, P.S., and Landhäusser, S.M. (2004). A method for routine measurements of total sugar and starch content in woody plant tissues. Tree Physiol. *24*, 1129–1136.

68. Landhäusser, S.M., Chow, P.S., Dickman, L.T., Furze, M.E., Kuhlman, I., Schmid, S., Wiesenbauer, J., Wild, B., Gleixner, G., Hartmann, H., et al. (2018). Standardized protocols and procedures can precisely and accurately quantify non-structural carbohydrates. Tree Physiol. *38*, 1764–1778.

69. Lamy, J.B., Delzon, S., Bouche, P.S., Alia, R., Vendramin, G.G., Cochard, H., and Plomion, C. (2014). Limited genetic variability and phenotypic plasticity detected for cavitation resistance in a Mediterranean pine. New Phytol. *201*, 874–886.

70. Spitze, K. (1993). Population structure in *Daphnia obtusa*: quantitative genetic and allozymic variation. Genetics *135*, 367–374.

71. Slater, L.J., Villarini, G., and Bradley, A.A. (2019). Evaluation of the skill of North-American Multi-Model Ensemble (NMME) Global Climate Models in predicting average and extreme precipitation and temperature over the continental USA. Clim. Dyn. *53*, 7381–7396.

72. Zhou, X., and Stephens, M. (2012). Genome-wide efficient mixed-model analysis for association studies. Nat. Genet. *44*, 821–824.

STAR★METHODS

KEY RESOURCES TABLE

REAGENT or RESOURCE	SOURCE	IDENTIFIER
Chemicals, Peptides, and Recombinant Proteins		
Acetic Acid	VWR	BDH20108.292
95% Ethanol	VWR	89125-180
Sodium Acetate	VWR	200004-240
Alpha-Amylase	Sigma Aldrich	A4551
Amyloglucosidase	Sigma Aldrich	1202332001
Phenol	VWR	BT135960-100G
Sulfuric Acid	VWR	BDH3072-2.5LG
PGO	Sigma Aldrich	P7119
O-dianisidine dihydrochloride	Sigma Aldrich	D3252
Deposited Data		
Total Nonstrucral Carbohydrate concentrations	This paper	https://github.com/blumsteinm/H2_Qst_Model
Populus trichocarpa sequence data	[42]	https://genome.jgi.doe.gov/portal/Poptr1_1/Poptr1_1.download.html
Climate Data of Western North America (WNA)	[50]	https://sites.ualberta.ca/~ahamann/data/climatewna.html
Software and Algorithms		
R v.3.5.1	[57]	https://www.r-project.org/
EMMAX	[58]	https://genome.sph.umich.edu/wiki/EMMAX
STAN/rstan v. 2.18.2	[59]	http://www.mc-stan.org
Vegan v.2.5-3 (R package)	[60]	https://cran.r-project.org/web/packages/vegan/vegan.pdf
Fields v.9.6	[61]	https://cran.r-project.org/web/packages/fields/index.html
Gamma hierarchical model	This paper	https://github.com/blumsteinm/H2_Qst_Model
topGO	[62]	https://bioconductor.org/packages/release/bioc/html/topGO.html
GOstats	[63]	https://bioconductor.org/packages/release/bioc/html/GOstats.html

LEAD CONTACT AND MATERIALS AVAILABILITY

Further information and requests for resources and reagents should be directed to and will be fulfilled by the lead contact, Meghan Blumstein (blumsteinm@gmail.com). All data and scripts generated by this study have been deposited in (https://github.com/blumsteinm/H2_Qst_Model).

EXPERIMENTAL MODEL AND SUBJECT DETAILS

Samples were collected from a Department of Energy black cottonwood (*Populus trichocarpa*) common garden, located near Clatskanie, Oregon (46.12°N, 123.27°W). The garden contains three randomized blocks of replicated genotypes along an East-West axis each containing 1,060 unique genotypes for a total of 3,180 individuals in each garden, which originate from 16 different provenances (referred to here as populations) (Figure 1). Population assignments were taken from a previous publication [64]. Plants in the garden received no extra water or nutrients after their establishment in the first year. The collection of each accession is described in Slavov et al. [39]. All individuals were planted in 2009, but one replicate was coppiced in the winter of 2013-2014, thus we only sampled from the two non-coppiced replicates where individuals were eight years old at the time of sampling

METHOD DETAILS

Field Collection

All samples were collected from January 6th to January 10th 2017, between 7a.m. and 4 p.m. While NSC concentrations are well known to fluctuate seasonally in predictable ways [38, 65], there is little evidence of diurnal fluctuations in total storage in woody

tissues, particularly in the dormant season. Carbohydrates may hydrolyze back and forth between sugar and starch over the course of the day in woody tissues, while the total amount of sugars remains largely unchanged [66]. However, to account for potential differences in time of sampling and microenvironment, we sampled in a randomized, hierarchical experimental design. The diameter at breast height (DBH) was also taken during this period, with the average measuring 155.2mm ± 46.9mm.

We collected above (stem) and below-ground (root) tissue using a 4.3mm increment borer (Haglöf Company Group, Långsele, Sweden). Stem tissue was taken at DBH and root tissue was taken from major coarse roots approximately 30cm away from the base of the tree. Samples were kept on dry ice in the field during collection, then shipped to Harvard University in Cambridge, MA and stored at −80°C.

Sampling was designed to collect a *minimum* of three unique genotypes (two replicates each) from each of the 16 populations, for a total of 96 initial trees sampled for assessment of heritability. An additional 220 individuals were collected to increase power for in the GWAS analysis for a total of 316 individuals from, representing 242 unique genotypes.

NSC Laboratory Preparation

We measured sugar and starch concentrations in the outer 2cm of the stem cores and outer 1.5cm of the root cores. Samples were first freeze-dried for 24-hours (FreeZone 2.5; Labconco, Kansas City, MO, and Hybrid Vacuum Pump, Vacuubrand, Wertheim, Germany), then ground to a fine powder (mesh 10, Thomas Scientific Wiley Mill, Swedesboro, NJ, USA; SPEX SamplePrep 1600; MiniG, Metuchen, NJ) and stored in sealed glass vials. Sugar and starch extraction protocols were adapted from [67]

Sugar was extracted from 10 mg of dried tissue using 80% hot ethanol, followed by a colorimetric assay with phenol and sulfuric acid, and read using a spectrophotometer at 490nm (Thermo Fisher Scientific GENESYS 10S UV-Vis, Waltham, MA). Sugar concentrations of mg sugar per g of dry wood were calculated using a 1:1:1 glucose-fructose-galactose standard curve (Sigma Chemicals, St. Louis, MO).

Starch was extracted using the tissue remaining after sugar extraction. Tissue was solubilized in NAOH, then incubated for 24-hours with alpha-amylase and amyloglucosidase digestive enzymes, which digested starch into glucose. Solutions were then assayed using a PGO-color reagent solution (Sigma chemicals) and read on the spectrophotometer at 525nm. Starch concentrations of mg glucose-starch-equivalent per g dry wood were calculated based on a glucose standard curve (Sigma Chemicals).

For all lab analyses, at least two internal laboratory standards were included (*Quercus rubrum* stemwood from Harvard Forest, MA; 42.01 ± 5.13 mg·g-1 Sugar, 30.17 ± 4.23 mg·g-1 starch). This acid methodology extracts all fructose, glucose, sucrose, and starch, as well as other oligosaccharides and other glucans [68]. We report these carbohydrates as one combined metric of Total Nonstructural Carbohydrates (TNC), representing sugar and starch concentrations added together.

QUANTIFICATION AND STATISTICAL ANALYSIS

Spatial Autocorrelation

Logged data were corrected for within-garden spatial autocorrelation using a thin-plate spline method (e.g., [64]), using the *fields* (9.6) package in *R* v.3.5.1 [57]. The model intercept was then added back to the residuals and then the exponential of these values was taken to place them back on a biologically meaningful scale.

Statistical Model

Given variation in our hierarchical sampling regime, we chose to use Bayesian hierarchical modeling to parse variation within and among populations. All statistical analyses were conducted in *R*, using the programming language *Stan* (http://www.mc-stan.org) [59], accessed via the *rstan* v.2.18.2 package. All model parameters were assigned noninformative priors (https://github.com/blumsteinm/H2_Qst_Model). We chose to treat both above and belowground stores as separate traits because they appear to vary independently in the literature [34, 35] and do not appear to tradeoff within other species [38] or across our populations. We also calculated the ratio of above to below-ground storage concentrations within trees and examined heritable variation in this trait. The ratio was calculated as the concentration of root storage minus the concentration of stem storage, divided by the larger of the two values.

Two different models were run to parse (1) the heritable variation and (2) the variation within and among populations (N_{stems} = 314, N_{roots} = 316). We chose to run two separate models for ease of extracting genetic variation values from the heritability model [e.g., 64, 69] The models took the form of the following hierarchical equations:

$$Y_{ig} = \alpha_g + \varepsilon_{ig} \quad (1)$$

$$Y_{igp} = \alpha_p + \alpha_{gp} + \varepsilon_{igp} \quad (2)$$

where *p* is population (i.e., provenance of genotype; N_{pop} = 16), g is genotype (N_g = 245), and *i* is individual. Both above and belowground data were modeled as a gamma distribution as they both had long right tails and no values at or below 0. The random effects outcomes ($\alpha's$) of Equations 1 and 2 were estimated using 6,000 random draws from the posterior distribution of each equation respectively, using the mean value of draw as each parameter estimate. These estimates for the heritable variation in storage are

also known as the best linear unbiased predictions (BLUPs). This method was also repeated with our diameter measurements to calculate the heritable variation in DBH.

Heritability, Q_{st}, and F_{st}

Both broad-sense heritability (H^2) and phenotypic divergence (Q_{st}) were estimated using the Bayesian hierarchical model outputs. Each parameter required for the H^2 and Q_{st} estimates were drawn from the posterior distributions of both Equations 1 and 2 and used to calculate H^2 and Q_{st} 6,000 times (for each of the posterior draws), generating uncertainty bounds for each estimate. H^2 was calculated using the random effects variances from Equation 1 as:

$$\sigma^2_{Genotype} \Big/ \left(\sigma^2_{Genotype} + \sigma^2_{Microenvironment}\right) \quad (3)$$

Genotype variance was taken as the variance among replicates and microenvironmental variance was taken as the residual variance of the model. Q_{st} was calculated via the formula [49, 70]:

$$\sigma^2_{Population} \Big/ \left(2\sigma^2_{Genotype} + \sigma^2_{Population}\right) \quad (4)$$

F_{st} estimates were taken from previous work [64], where F_{st} was calculated in 1-kb windows as $(\pi_T\text{-}\pi_S)/\pi_T$; where π_T is SNP diversity across all individuals and π_S is weighted within-population SNP diversity. A nonparametric Wilcoxon t test was performed to test whether the distribution of F_{st} values and above and belowground Q_{st} posterior estimates significantly differed. All results are reported in text.

Climate

The past climatic data used to estimate clinal variation in NSC storage were climate-normal layers fit to western North America that represent 30-year normals (1961-1990) from climateWNA [50]. We chose this dataset in particular because the down-scaling routine is optimized for our study region and like-formatted (ie. scale and variables) climate projections were available for a multitude of GCMs and climate scenarios, allowing us to project the environmental clines we identified into future climate space. However, by using Normals data, we do lose many variables that go beyond means to capture climate stochasticity. All 26 available climate parameters were highly correlated, thus to reduce dimensionality and account for collinearity among our climatic variables, we used a principle components analysis (PCA) (Figure 2). Many climate parameters were found to be redundant in our PCA given their high correlation with other parameters and all parameters analyzed fell along a precipitation or temperature gradient. Thus, we chose to include only the 8 climate variables with the highest loading values on PC1 and PC2 in our analysis to simplify visualization (Figure 2).

We then fitted above and belowground NSC storage concentrations population-level heritable variation to the first two principle components of this ordination space using ''envfit'' from the *vegan* v.2.5-3 package [60] and patterns were further teased out using a linear regression of population-variation against PC1and PC2 as predictors (Figure 2, N = 16).

To get population-level estimates of future climate, we used down-scaled data representing the IPCC's A1B (moderate) emissions scenario from the National Center for Atmospheric Research's CCSM3 global climate model for the year 2080 from climateWNA [50]. We chose to run NCAR's CCSM3 model as it is part of the North American Multi-Model Ensemble and had available data on climateWNA. CCSM3 predictions are in line with other models in the North American Multi-Model Ensemble as well as the ensemble predictions [71]. Once acquired, we projected future climate predictions into the PC space fit with current climate and used these values to assess climate response (Figure 3). In addition, we repeated our analyses using ensemble data for all 23 CMIP3 models from climateWNA and found no significant differences in our predictions (Figure S4).

Genome-Wide Association Study & Gene Ontology

We performed a genome-wide association study (GWAS) on the spatial-autocorrelation corrected values of heritable variation for both above and belowground total NSC storage concentrations following the protocol of Zhang et al. [58] and the software *EMMAX* with a correction for kinship [72]. We utilized 8,253,066 SNP variants with dataset-wide minor allele frequencies > 0.05, from 917 accessions, using -log10(P) > = 5 as our inclusion cutoff (Figure 4). We also repeated analyses with more stringent multiple-testing FDR rate corrections (-log10 = 6 and 6.5) and found them to be robust, but chose to use the threshold of -log10 = 5 given the likely polygenic nature of the trait and to more robustly build predictive models. Our analysis uncovered several gene models within 6kb (the distance at which LD decays in populus [42]) of SNPs with p values above our inclusion cutoff with functions purportedly associated with carbohydrate synthesis, binding, and transport in both stems, such as Potri.001G134900, Potri.001G226600 and Potri.003G022900, and roots, such as Potri.006G122000, Potri.007G040700, Potri.011G110800 (Table S1). Gene models associated with the production/degradation of secondary compounds and lipids were also uncovered (Table S1). We then performed a gene ontology (GO) analysis to summarize these results, then aggregate results into GO slim categories (Figure S2). We used the packages *topGO* version 1.0 [62] and *GOstats* version 1.7.4 in R [63] and the *P. trichocarpa* v.3.1 annotation file from the DOE repository to conduct the analysis [42, 64].

Minor Allele Frequency Projections

At each locus associated with aboveground or belowground storage, we calculated the minor allele frequency (MAF) by population. We then generated a statistical association between the MAF of each population at each locus associated with NSC storage and the PCs defined in our previous climate analysis via a canonical correlation analysis (CCA) with 4,000 permutations, running above and belowground loci in separate analyses. CCA is a multivariate method commonly used in community ecology to establish relationships between biological assemblages of species and environment, where here each loci is acting like species. We checked the accuracy of our model by plotting predicted allele frequencies against actual by population, finding (Figure S3). We then predicted the expected population-level MAF at each locus given the CCA model and 2080 projected climate PCs for each population. Finally, to make interpolated maps of our population-level data for ease of viewing, we used a thin-plate spline method from the *fields v.9.6* package in *R [*61*]* (all results in Figure 4). We also repeated this analysis using genes with representative SNPs, meaning we chose the most significant SNP from each gene to use as the marker for each gene region.

DATA AND CODE AVAILABILITY

The datasets and code generated during this study are available on github (https://github.com/blumsteinm/H2_Qst_Model).